

# A Comprehensive Structure–Function Analysis of *Arabidopsis* SNI1 Defines Essential Regions and Transcriptional Repressor Activity

Rebecca A. Mosher,<sup>1</sup> Wendy E. Durrant, Dong Wang, Junqi Song, and Xinnian Dong<sup>2</sup>

Developmental, Cell, and Molecular Biology Group, Department of Biology, Duke University, Durham, North Carolina 27708

The expression of systemic acquired resistance (SAR) in plants involves the upregulation of many *Pathogenesis-Related* (*PR*) genes, which work in concert to confer resistance to a broad spectrum of pathogens. Because SAR is a costly process, SAR-associated transcription must be tightly regulated. *Arabidopsis thaliana* SNI1 (for Suppressor of NPR1, Inducible) is a negative regulator of SAR required to dampen the basal expression of *PR* genes. Whole genome transcriptional profiling showed that in the *sni1* mutant, Nonexpresser of *PR* genes (*NPR1*)–dependent benzothiadiazole S-methylester–responsive genes were specifically derepressed. Interestingly, SNI1 also repressed transcription when expressed in yeast, suggesting that it functions as an active transcriptional repressor through a highly conserved mechanism. Chromatin immunoprecipitation indicated that histone modification may be involved in SNI1-mediated repression. Sequence comparison with orthologs in other plant species and a saturating NAAIRS-scanning mutagenesis of SNI1 identified regions in SNI1 that are required for its activity. The structural similarity of SNI1 to Armadillo repeat proteins implies that SNI1 may form a scaffold for interaction with proteins that modulate transcription.

## INTRODUCTION

Plants possess a number of defense mechanisms to combat pathogen attacks. Systemic acquired resistance (SAR) is a broad-range resistance to viral, bacterial, fungal, and oomycete pathogens that can be induced after a local infection (Ryals et al., 1996; Sticher et al., 1997; Durrant and Dong, 2004). During the onset of SAR, salicylic acid (SA) levels increase in both local and systemic tissues, causing upregulation of *Pathogenesis-Related* (*PR*) genes (Van Loon and Van Strien, 1999). These genes encode secreted or vacuole-targeted proteins with antimicrobial activities. This leads to the hypothesis that *PR* proteins form a defensive shield in systemic tissues and prevent pathogens from establishing an infection. Because overexpression of a single *PR* protein is not sufficient to establish broad-spectrum resistance (Brogie et al., 1991; Liu et al., 1994; Zhu et al., 1994), it is believed that *PR* proteins enhance resistance by working in concert (Zhu et al., 1994).

The massive expression and export of *PR* proteins significantly tax the plant's resources (Heidel et al., 2004). Repeated induction of SAR in *Arabidopsis thaliana* has a fitness cost (Heil et al., 2000). Many mutants with constitutive SAR have decreased stature,

decreased fertility and seed set, and spontaneous cell death (Bowling et al., 1994, 1997; Hunt et al., 1997; Clarke et al., 1998, 2000, 2001; Maleck et al., 2002). Some of these mutants also have increased susceptibility to necrotrophic pathogens, because the high levels of SA found in these mutants inhibit jasmonate-mediated resistance to such pathogens. The inducible nature of SAR allows a plant to activate the response only when the risk of infection outweighs the cost of resistance. Therefore, it is not surprising that the transcription of *PR* genes is tightly regulated by both positive and negative factors.

Several approaches have been used to study the regulation of *PR* genes. Linker-scanning mutagenesis of the *PR-1* promoter identified two *as-1* elements and one W box as strong positive, weak negative, and strong negative *cis* elements, respectively (Lebel et al., 1998). Microarray analysis identified 31 genes coordinately regulated with *PR-1* (Maleck et al., 2000). The *as-1* element was found in more than half of these genes' promoters, and W boxes were overrepresented. The abundance of W boxes in the promoters of the *PR-1* regulon genes and the negative role of the W box in the *PR-1* promoter suggest that transcriptional derepression may be critical for SAR activation.

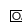
Genetic screens identified *NPR1/NIM1* (for Nonexpresser of *PR* genes/No Immunity; hereafter referred to as *NPR1*) as a key positive regulator of SAR (Cao et al., 1994; Delaney et al., 1995). Mutant *npr1* plants exhibit neither systemic *PR* gene expression nor resistance in response to pathogen induction or SA treatment. *NPR1* is regulated posttranslationally to activate *PR* gene expression. Upon induction, monomeric *NPR1* is released from a large oligomeric complex and translocates to the nucleus (Mou et al., 2003), where it interacts with members of the TGA group of transcription factors (Zhang et al., 1999; Després et al., 2000; Zhou et al., 2000). TGA factors bind different *as-1* elements to play both positive and negative roles in controlling *PR* gene

<sup>1</sup> Current address: Sainsbury Laboratory, Norwich NR4 7UH, UK.

<sup>2</sup> To whom correspondence should be addressed. E-mail xdong@duke.edu; fax 919-613-8177.

The author responsible for distribution of materials integral to the findings presented in this article in accordance with the policy described in the Instructions for Authors (www.plantcell.org) is: Xinnian Dong (xdong@duke.edu).

 Online version contains Web-only data.

 Open Access articles can be viewed online without a subscription. Article, publication date, and citation information can be found at www.plantcell.org/cgi/doi/10.1105/tpc.105.039677.

expression (Pontier et al., 2001). Consistent with the result of linker-scanning mutagenesis of the *PR-1* promoter, deletion of *TGA2*, *TGA5*, and *TGA6* in the same plant not only abolished the inducibility of *PR* genes but also increased the basal expression of these genes (Zhang et al., 2003).

In addition to positive regulators, a negative regulator of *PR* genes, *sni1* (for *suppressor of npr1, inducible*), was identified in a screen for suppressors of *npr1* (Li et al., 1999). The *npr1 sni1* double mutant regains SA-inducible *PR* gene expression and resistance. Moreover, in both the *sni1* and *npr1 sni1* mutants, background levels of *PR* genes are increased. Similar to mutants with constitutive *PR* gene expression, *sni1* exhibits pleiotropic phenotypes that include decreased leaf size, altered leaf texture, decreased apical dominance, and greatly reduced root length (Li et al., 1999; X. Li and X. Dong, unpublished data). The SNI1 protein, which lacks sequence similarity to any known protein or domain, is hypothesized to function in the nucleus as a transcriptional repressor of *PR* genes. After induction, SNI1 repression is removed, perhaps through the function of NPR1.

In this study, we show that the SNI1 protein accumulates in the nucleus. Through genome-wide transcriptional profiling, we found that knocking out *SNI1* function causes specific derepression of NPR1-dependent benzothiadiazole S-methyl ester (BTH)-responsive genes. Transcriptional assays in yeast and chromatin immunoprecipitation in *Arabidopsis* suggest that SNI1 represses transcription by a highly conserved mechanism that affects chromatin modification. Sequence comparison with orthologs in other plant species and saturating NAAIRS-scanning mutagenesis of SNI1 defined regions in the protein that are required for its activity. Three-dimensional localization of these residues on a predicted structure supports the hypothesis that SNI1 serves as a protein scaffold, interacting with transcription factors or histone-modifying enzymes to repress defense genes.

## RESULTS

### SNI1 Is Primarily Localized in the Nucleus

Although hypothesized to function in the nucleus, the SNI1 sequence has no discernible nuclear localization signal. Biolistic transformation of *P<sub>35S</sub>::SNI1-GFP* into onion (*Allium cepa*) epidermal cells showed nuclear fluorescence, indicating that this fusion protein can be localized in the nucleus (Li et al., 1999). To determine the subcellular localization of functional SNI1 in planta, we made an N-terminal fusion of green fluorescent protein (GFP) to SNI1 and expressed this protein using the 35S promoter in the *sni1-1* mutant. The functionality of this fusion protein was confirmed by complementation of the phenotype conferred by *sni1*: restoration of wild-type leaf morphology, elimination of background *P<sub>BGL2</sub>::GUS* (for  $\beta$ -glucuronidase) reporter expression, wild-type induction of *P<sub>BGL2</sub>::GUS*, and restoration of wild-type root length (Figures 1A to 1C). Immunoblot analysis of independent transgenic lines detected the fusion protein in only two lines, indicating that although all lines showed complementation of the phenotype conferred by *sni1*, most did not accumulate a detectable amount of the protein. These two *P<sub>35S</sub>::SNI1-GFP* lines were then analyzed for the subcellular

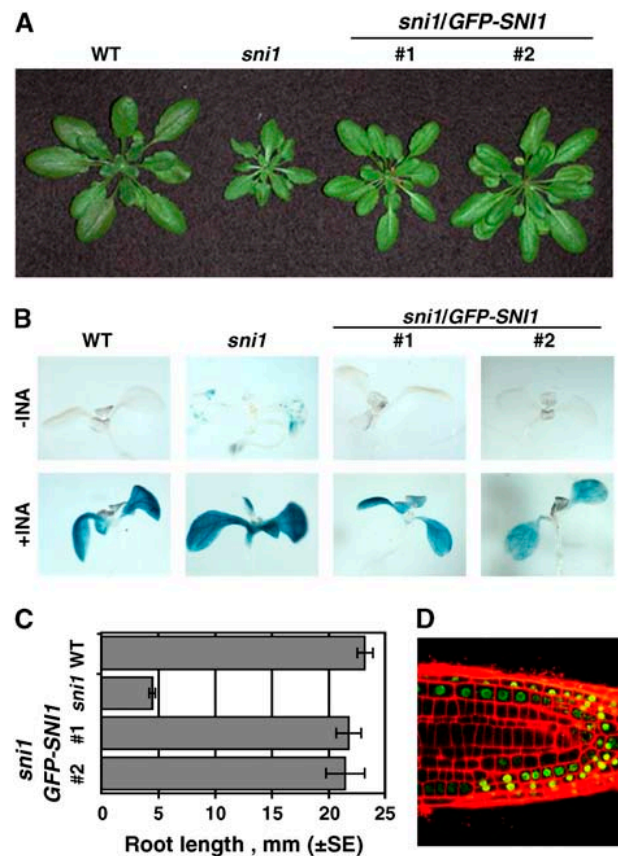


**Figure 1.** GFP-SNI1 Is Localized in the Nucleus.

(A) *P<sub>35S</sub>::GFP-SNI1* transgenic lines (GFP-SNI1 plants 1 and 2) show complementation of the *sni1-1* leaf morphology. Plants were soil-grown for 4 weeks.

(B) *P<sub>35S</sub>::GFP-SNI1* transgenic lines show complementation of the *sni1-1* mutation in *P<sub>BGL2</sub>::GUS* gene expression. Seedlings were grown on MS plates with (+) or without (−) INA (10  $\mu$ M) for 12 d and stained for GUS activity (Bowling et al., 1994).

(C) *P<sub>35S</sub>::GFP-SNI1* transgenic lines show complementation of the *sni1-1* mutation in root length. Root length was measured on 8-d-old plate-grown seedlings. For each genotype, 15 seedlings were measured, and SE values were calculated from results of three independent experiments.

(D) GFP-SNI1 is primarily localized in the nucleus. *P<sub>35S</sub>::GFP-SNI1* seedlings were grown vertically on MS plates for 5 d. Roots were treated with propidium iodide to stain cell walls before microscopy. A  $\times 60$  water-immersion lens and a 488-nm laser were used with a laser-scanning confocal microscope. GFP fluorescence was false-colored green and propidium iodide was false-colored red.

localization of GFP fluorescence using confocal microscopy. Because of the low expression levels of the transgene, we chose to use root tissues in which chlorophyll fluorescence is absent. In both lines, the predominant fluorescence was nuclear, with some fluorescent loci peripheral to the nucleus (Figure 1D). Transgenic lines carrying *P<sub>35S</sub>::GFP* in the same vector showed diffuse nuclear and cytoplasmic fluorescence, as the GFP was below the size-exclusion limit of nuclear pores (data not shown). The localization and intensity of GFP-SNI1 fluorescence did not

change when seedlings were grown in the presence of 10  $\mu$ M 2,6-dichloroisonicotinic acid (INA) (data not shown).

### The *sni1* Mutation Causes Specific Derepression of NPR1-Dependent BTH-Responsive Genes

The SNI1 protein is hypothesized to be a transcriptional repressor of *PR* genes because the *sni1* mutation not only restores the inducibility of the *PR-1* and *PR-2* (*BGL2*) genes in *npr1* but also causes increased background expression of these genes in the absence of an inducing signal. To determine the degree and specificity of the mutation on global transcription, microarray analysis was conducted with RNA from wild-type and *sni1-1* plants using the Affymetrix 24,000 gene chip, ATH1. The resulting expression profiles from three independent biological replicates were analyzed using mixed-model analysis of variance (ANOVA) with multiple testing correction to adjust for type I family-wise error to acquire *q* values (Levesque et al., 2006). We found that the levels of 95 transcripts were consistently increased in *sni1* compared with the wild type (Table 1), whereas 4 genes were consistently reduced compared with the wild type (*q* value < 0.05, fold change > 2). An analysis of gene ontology terms identified functional classes significantly overrepresented in the genes derepressed in *sni1* (see Supplemental Table 1 online). As expected, genes involved in the response to biotic stimulus are the most prominent among this group. To determine the relationship between SNI1 and NPR1, we performed another microarray experiment using the Affymetrix 24,000 gene chip (ATH1) in both the wild type and *npr1-1* to identify BTH-responsive genes and NPR1-dependent genes. Four-week-old soil-grown plants were sprayed with 60  $\mu$ M BTH, and tissue was collected in triplicate at 0, 8, and 24 h. Using the same analytical tools, we found that 88 (93%) of the 95 genes derepressed in *sni1* were regulated by BTH (*q* value < 0.05 for at least one time point) and even more strikingly that 90 (95%) of the 95 genes derepressed in *sni1* were NPR1-dependent (*q* value < 0.05 for at least one time point). These data strongly support our hypothesis that SNI1 functions in the NPR1 signaling pathway.

### SNI1 Functions as a Transcription Repressor in a Yeast Expression System

Several failed attempts to identify SNI1 interactors using yeast two-hybrid screens suggested that SNI1 might have transcriptional repressor activity in yeast and was preventing expression of the reporter genes by the bait-prey complex. To test this hypothesis, a yeast transcriptional assay was conducted. SNI1 was fused to the Gal4 DNA binding domain (G4DBD) and expressed in a yeast strain carrying the transcriptional reporter SS38 (Figure 2A). This reporter contains five copies of the Gal4 UAS upstream of two copies of the constitutive GCN4 promoter, which drives expression of the *LacZ* gene encoding  $\beta$ -galactosidase. In this system, transcription of *LacZ* can be further activated or repressed by the binding of transcriptional regulators to the Gal4 UAS through fusion with G4DBD (Saha et al., 1993). As shown in Figure 2B, expression of G4DBD-SNI1 (at a comparable level to G4DBD [Figure 2C]) caused a threefold reduction in reporter expression compared with the G4DBD

control, confirming that SNI1 indeed has transcriptional repressor activity in yeast. Detection of repressor activity across kingdoms and at diverse promoters suggests that SNI1 inhibits transcription through a highly conserved active mechanism such as chromatin modification or remodeling.

### Loss of *SNI1* Function Leads to Chromatin Modifications at the *PR-1* Promoter That Mimic Induction

To investigate the role of histone modification in the regulation of *PR* gene transcription, we conducted chromatin immunoprecipitation. Within the standard histone code, acetylation of histone H3 (AcH3) and dimethylation of Lys-4 of histone H3 (MeH3K4) are associated with active chromatin and transcription (Strahl and Allis, 2000; Zhang and Reinberg, 2001). To measure the amount of *PR-1* promoter associated with active chromatin, AcH3 and MeH3K4 were immunoprecipitated from cross-linked extracts and the associated DNA was purified and subjected to quantitative PCR. Specifically, a region of the *PR-1* promoter containing known *cis* elements was examined (Figure 3A). As expected, there was a significant increase in AcH3 and MeH3K4 modifications at the *PR-1* promoter concurrent with the induction of transcription by BTH (Figure 3B). Interestingly, in the *sni1* mutant, the *PR-1* promoter was associated with high levels of AcH3 and MeH3K4 even before induction. Two-tailed *t* tests showed that there is no significant difference between the levels of MeH3K4 or AcH3 modifications in induced wild type and *sni1* with or without induction, indicating that loss of SNI1 activity is the cause of this chromatin change during induction.

### SNI1 Is a Plant-Specific Protein with Conserved Function

SNI1 has no significant sequence similarity to proteins of known function. We previously reported a similarity to the N-terminal domain of the tumor suppressor, retinoblastoma (Rb), but the similarity was weak (Li et al., 1999). Since then, ESTs encoding possible SNI1 orthologs from many plant species have been deposited in public databases and identified using TBLASTN to search the National Center for Biotechnology Information (NCBI) EST database (see Supplemental Table 2 online) (Altschul et al., 1997). Both monocots and dicots are represented among the ESTs, and sequences from two spruce species indicate that SNI1 orthologs may also exist in conifers. No nonplant orthologs have been identified.

To further investigate these ESTs, full-length cDNAs from soybean (*Glycine max*) and potato (*Solanum tuberosum*) were cloned through 5' and 3' RNA ligase-mediated rapid amplification of cDNA ends. ESTs encoding complete or nearly complete SNI1 proteins were found in NCBI for *Medicago truncatula*, barley (*Hordeum vulgare*), and noble cane (*Saccharum officinarum*). A search of the draft rice (*Oryza sativa*) genome using the GeneFinder software (C. Wilson, L. Hilyer, and P. Green, unpublished data; <http://ftp.genome.washington.edu/cgi-bin/GeneFinder>) and knowledge of the *Arabidopsis* SNI1 intron/exon structure identified one locus that encodes Os *Sni1*. Queries of the high-throughput genome sequences of lotus (*Lotus japonicus*) also identified a genomic locus (Lj *Sni1*). Gene prediction for this locus was based upon the high similarity between soybean

**Table 1.** Genes with Higher Expression in *sn1* Than in the Wild Type

Affymetrix Number	Locus	Name and Description	Log <sub>2</sub> Ratio	q Value	BTH-Responsive in the Wild Type (q Value)		NPR1 Dependence (q Value)	
					8 h	24 h	8 h	24 h
AFFX-r2-At-U12639_at		BGL2 promoter:GUS reporter	2.2	4.84E-13	1.37E-05	3.96E-26	9.10E-07	1.49E-27
251625_at	At3g57260	BGL2, $\beta$ -1,3-glucanase 2 (PR-2)	3.6	3.32E-19	3.63E-08	1.97E-23	3.15E-07	9.74E-07
266070_at	At2g18660	EXPR3, expansin-related protein 3	2.9	3.85E-41	1.03E-38	5.72E-74	7.73E-41	3.19E-61
254265_s_at	At4g23140	CRK6/RLK5, Cys-rich receptor-like protein kinase	2.5	2.45E-13	1.83E-12	4.33E-27	5.33E-15	5.59E-13
262119_s_at	At1g02930	ATGSTF6/GST1/ERD11	2.2	1.80E-17	7.76E-06	7.63E-19	2.25E-10	5.04E-16
	At1g02920	(At1g02930) ATGSTF7/GST11 (At1g02920)						
260568_at	At2g43570	Chitinase, putative	2.2	8.08E-16	7.16E-26	4.42E-30	1.26E-21	1.23E-12
263539_at	At2g24850	Aminotransferase, putative	2.1	9.69E-07	1.24E-11	8.79E-27	4.25E-16	1.82E-16
250445_at	At5g10760	Aspartyl protease family protein	2.1	1.50E-16	4.48E-15	3.58E-22	4.52E-15	2.35E-15
264635_at	At1g65500	Expressed protein	1.9	9.12E-29	6.35E-02 <sup>a</sup>	1.30E-03	1.05E-02	2.54E-01 <sup>a</sup>
257365_x_at	At2g26020	Plant defensin protein, putative (PDF1.2b)	1.9	9.51E-04	1.05E-04	8.60E-08	1.54E-05	6.94E-04
266385_at	At2g14610	PR-1	1.9	2.64E-07	5.06E-21	1.49E-37	4.77E-27	1.08E-43
259925_at	At1g75040	PR-5	1.8	9.69E-10	3.19E-15	4.77E-37	4.45E-09	3.92E-14
264958_at	At1g76960	Expressed protein	1.8	1.51E-08	2.60E-11	1.39E-18	7.19E-12	7.33E-06
250435_at	At5g10380	Zinc finger (C3HC4-type RING finger) family protein	1.7	5.34E-15	3.05E-21	3.97E-39	9.41E-17	4.67E-19
249754_at	At5g24530	Oxidoreductase, 2OG-Fe(II) oxygenase family protein	1.7	3.81E-10	5.10E-17	2.09E-29	9.37E-21	6.34E-18
248322_at	At5g52760	Heavy metal-associated domain-containing protein	1.7	1.42E-07	2.45E-11	1.26E-36	3.21E-07	7.94E-16
265058_s_at	At1g52030	Myrosinase binding protein, putative (F-ATMBP)	1.7	6.69E-04	2.62E-02	6.64E-02 <sup>a</sup>	1.88E-02	7.18E-01 <sup>a</sup>
258791_at	At3g04720	PR4/HEL, similar to the antifungal protein hevein	1.7	1.92E-05	1.77E-01 <sup>a</sup>	3.36E-02	4.67E-02	5.00E-02 <sup>a</sup>
267546_at	At2g32680	Disease resistance family protein, contains Leu-rich repeat domains	1.6	1.12E-10	1.10E-05	8.68E-12	2.44E-02	7.73E-01 <sup>a</sup>
252234_at	At3g49780	Phytosulfokines 3 (PSK3)	1.6	9.78E-10	3.98E-11	2.32E-16	2.47E-08	9.31E-04
256337_at	At1g72070	DNAJ heat-shock N-terminal domain-containing protein	1.6	1.33E-05	1.22E-11	2.71E-28	1.92E-11	1.51E-18
256596_at	At3g28540	AAA-type ATPase family protein	1.5	1.29E-06	4.79E-02	2.40E-04	5.90E-03	8.75E-02 <sup>a</sup>
249052_at	At5g44420	Plant defensin protein, putative (PDF1.2a)	1.5	2.31E-03	2.04E-17	1.07E-30	1.03E-16	7.02E-17
265053_at	At1g52000	Jacalin lectin family protein	1.5	1.00E-03	1.32E-24	3.53E-36	3.51E-27	4.29E-20
266017_at	At2g18690	Expressed protein	1.5	9.28E-07	8.93E-14	1.82E-27	3.20E-12	2.07E-14
249983_at	At5g18470	Curculin-like (mannose binding) lectin family protein	1.5	6.76E-06	3.12E-12	2.05E-22	1.36E-14	2.13E-19
259272_at	At3g01290	Band 7 family protein	1.5	1.39E-09	1.25E-33	2.33E-43	6.77E-32	8.38E-13
254869_at	At4g11890	Protein kinase family protein	1.5	3.76E-06	9.33E-04	4.57E-04	8.67E-05	1.11E-05
252170_at	At3g50480	HR4, homolog of resistance protein RPW8	1.5	1.26E-13	2.45E-11	2.37E-26	8.42E-13	3.52E-20
261692_at	At1g08450	CRT3, calreticulin 3	1.4	3.27E-12	1.45E-21	2.66E-34	5.43E-18	2.26E-12
254271_at	At4g23150	Ser/Thr protein kinase	1.4	7.89E-13	2.56E-13	2.38E-24	1.13E-18	4.47E-14
245329_at	At4g14365	C3HC4-type RING finger family/ankyrin repeat family protein	1.4	1.34E-06	5.66E-02 <sup>a</sup>	2.31E-04	3.92E-02	7.62E-01 <sup>a</sup>
260943_at	At1g45145	AtTRX5, cytosolic thioredoxin	1.4	7.98E-06	1.05E-12	1.66E-41	4.13E-15	1.18E-33
260919_at	At1g21520	Expressed protein	1.4	1.05E-08	2.41E-01 <sup>a</sup>	2.04E-01 <sup>a</sup>	8.95E-02 <sup>a</sup>	6.53E-01 <sup>a</sup>
249346_at	At5g40780	LHT1, Lys- and His-specific transporter	1.4	1.65E-08	9.14E-03	4.61E-06	3.68E-02	2.15E-02
260556_at	At2g43620	Chitinase, putative	1.4	2.34E-12	1.36E-14	1.52E-19	3.93E-12	3.71E-06
263046_at	At2g05380	Gly-rich protein (GRP3S)	1.4	1.43E-05	1.96E-27	4.51E-47	3.89E-25	2.03E-27

(Continued)

**Table 1.** (continued).

Affymetrix Number	Locus	Name and Description	Log <sub>2</sub> Ratio	q Value	BTH-Responsive in the Wild Type (q Value)		NPR1 Dependence (q Value)	
					8 h	24 h	8 h	24 h
253666_at	At4g30270	Xyloglucan endo-1, 4-β-D-glucanase (SEN4, MERI-5)	1.4	1.70E-02	8.32E-02 <sup>a</sup>	1.32E-01 <sup>a</sup>	1.26E-01 <sup>a</sup>	3.72E-02
255479_at	At4g02380	Late embryogenesis abundant 3 family protein	1.3	1.95E-03	2.23E-01	1.71E-01	1.97E-01	3.34E-01 <sup>a</sup>
257623_at	At3g26210	CYP71B23, putative cytochrome P450	1.3	2.72E-09	1.65E-21	1.11E-25	1.63E-18	5.35E-11
259841_at	At1g52200	Expressed protein	1.3	6.69E-04	9.23E-21	5.20E-32	4.06E-21	2.58E-15
262832_s_at	At1g14870	Expressed protein, similar to PGPS/D12 ( <i>Petunia</i> × <i>hybrida</i> )	1.3	1.04E-04	1.10E-09	7.83E-15	7.73E-13	1.58E-06
245885_at	At5g09440	Phosphate-responsive protein, putative	1.3	2.14E-02	8.60E-25	3.37E-25	1.77E-30	6.77E-18
263478_at	At2g31880 At2g31890	Leu-rich repeat transmembrane protein kinase	1.3	4.14E-09	1.12E-19	9.93E-35	5.66E-17	5.57E-12
263783_at	At2g46400	WRKY46, WRKY transcription factor, group III	1.3	9.65E-16	9.80E-14	3.48E-31	9.68E-12	3.53E-13
263584_at	At2g17040	ANAC036, no apical meristem family protein	1.3	2.03E-05	1.56E-27	5.40E-59	1.28E-19	1.01E-46
264434_at	At1g10340	Ankyrin repeat family protein	1.3	6.01E-11	1.56E-27	1.08E-52	1.43E-31	1.11E-40
245038_at	At2g26560	Patatin, putative	1.2	3.16E-03	5.33E-13	6.00E-18	1.01E-11	3.79E-04
259655_at	At1g55210	Disease resistance response protein-related/ dirigent protein-related	1.2	3.04E-11	2.58E-14	6.68E-25	2.98E-14	1.24E-07
254231_at	At4g23810	WRKY53, WRKY transcription factor, group III	1.2	8.47E-03	1.94E-38	1.16E-54	7.66E-38	3.59E-39
248551_at	At5g50200	WR3, involved in jasmonate- independent wound signal transduction	1.2	3.11E-23	1.36E-04	8.24E-10	9.80E-07	1.39E-05
249581_at	At5g37600	Gln synthetase, putative	1.2	6.53E-03	1.77E-11	2.86E-17	1.61E-11	2.67E-12
262177_at	At1g74710	Isochorismate synthase 1 (ICS1)	1.2	1.86E-10	2.60E-09	1.73E-28	2.77E-08	5.32E-18
255524_at	At4g02330	Pectinesterase family protein	1.2	3.82E-09	1.01E-22	1.17E-54	9.10E-21	1.01E-46
248327_at	At5g52750	Heavy metal-associated domain-containing protein	1.2	1.73E-04	7.90E-16	5.28E-25	2.87E-13	8.34E-15
266371_at	At2g41410	Calmodulin, putative	1.2	2.06E-04	2.29E-01 <sup>a</sup>	1.42E-01 <sup>a</sup>	1.20E-01 <sup>a</sup>	5.17E-01 <sup>a</sup>
261339_at	At1g35710	Leu-rich repeat transmembrane protein kinase, putative	1.2	1.47E-02	4.31E-09	1.66E-30	1.83E-11	3.76E-29
252131_at	At3g50930	AAA-type ATPase family protein	1.2	5.66E-06	1.87E-01 <sup>a</sup>	2.05E-17	3.79E-02	7.52E-08
266292_at	At2g29350	SAG13, senescence-associated gene 13, short-chain alcohol dehydrogenase	1.2	1.70E-03	1.67E-11	1.01E-17	1.76E-12	2.14E-09
251673_at	At3g57240	Similar to glycosyl hydrolase family 17 protein	1.2	1.26E-02	7.69E-05	9.41E-39	1.08E-03	8.53E-33
259550_at	At1g35230	AGP5, arabinogalactan protein	1.2	1.23E-07	1.48E-02	3.34E-16	2.08E-04	2.21E-18
252417_at	At3g47480	Calcium binding EF hand family protein	1.2	1.59E-11	2.72E-09	1.68E-20	2.24E-09	1.77E-08
267083_at	At2g41100	TCH3, calmodulin-like protein, induced by touch and darkness	1.2	6.69E-05	1.32E-17	6.63E-27	6.44E-14	1.67E-04
254573_at	At4g19420	Pectinacetylsterase family protein	1.1	3.84E-02	1.52E-16	3.31E-40	2.75E-14	7.68E-29
246405_at	At1g57630	Disease resistance protein (TIR class), putative	1.1	4.35E-04	3.37E-14	7.93E-25	1.24E-14	3.29E-14
247327_at	At5g64120	Peroxidase	1.1	8.01E-07	1.26E-01 <sup>a</sup>	1.97E-01 <sup>a</sup>	2.84E-02	5.98E-01 <sup>a</sup>

(Continued)

**Table 1.** (continued).

Affymetrix Number	Locus	Name and Description	Log <sub>2</sub> Ratio	q Value	BTH-Responsive in the Wild Type (q Value)		NPR1 Dependence (q Value)	
					8 h	24 h	8 h	24 h
<b>250994_at</b>	<b>At5g02490</b>	<b>Heat-shock cognate 70-kD protein 2 (HSC70-2)</b>	<b>1.1</b>	<b>3.77E-11</b>	<b>1.63E-10</b>	<b>3.31E-40</b>	<b>1.65E-15</b>	<b>7.41E-35</b>
259609_at	At1g52410	Caldesmon-related	1.1	8.92E-04	1.85E-16	7.10E-31	2.49E-14	4.58E-26
259640_at	At1g52400	$\beta$ -Glucosidase, putative (BG1)	1.1	3.04E-02	1.07E-04	2.94E-35	4.79E-07	2.92E-32
<b>254387_at</b>	<b>At4g21850</b>	<b>Met sulfoxide reductase domain-containing protein/ SelR domain-containing protein</b>	<b>1.1</b>	<b>1.50E-16</b>	<b>1.23E-01<sup>a</sup></b>	<b>4.57E-04</b>	<b>5.87E-02<sup>a</sup></b>	<b>6.05E-01<sup>a</sup></b>
<b>248932_at</b>	<b>At5g46050</b>	<b>Proton-dependent oligopeptide transport (POT) family protein</b>	<b>1.1</b>	<b>4.18E-08</b>	<b>5.60E-21</b>	<b>1.11E-38</b>	<b>5.43E-18</b>	<b>5.07E-16</b>
<b>254975_at</b>	<b>At4g10500</b>	<b>Oxidoreductase, 2OG-Fe(II) oxygenase family protein</b>	<b>1.1</b>	<b>4.61E-11</b>	<b>8.60E-25</b>	<b>1.93E-63</b>	<b>3.37E-27</b>	<b>4.53E-50</b>
<b>256366_at</b>	<b>At1g66880</b>	<b>Ser/Thr protein kinase</b>	<b>1.1</b>	<b>1.49E-03</b>	<b>7.50E-10</b>	<b>1.37E-21</b>	<b>6.43E-11</b>	<b>4.79E-11</b>
<b>254784_at</b>	<b>At4g12720</b>	<b>MutT/nudix family protein</b>	<b>1.1</b>	<b>4.59E-09</b>	<b>1.94E-02</b>	<b>6.09E-03</b>	<b>1.53E-02</b>	<b>7.22E-03</b>
<b>258277_at</b>	<b>At3g26830</b>	<b>PAD3, cytochrome P450 required for synthesis of the phytoalexin camalexin</b>	<b>1.1</b>	<b>1.76E-05</b>	<b>6.39E-04</b>	<b>5.78E-02<sup>a</sup></b>	<b>2.41E-02</b>	<b>5.57E-01<sup>a</sup></b>
<b>267300_at</b>	<b>At2g30140</b>	<b>UDP-glucuronosyl/UDP-glucosyl transferase family protein</b>	<b>1.1</b>	<b>7.63E-05</b>	<b>1.78E-24</b>	<b>8.24E-32</b>	<b>4.35E-21</b>	<b>1.45E-24</b>
256603_at	At3g28270	Expressed protein, similar to At14a protein	1.1	4.78E-03	1.16E-12	8.29E-19	1.56E-14	1.27E-09
<b>246927_s_at</b>	<b>At5g25250</b>	<b>Expressed protein</b>	<b>1.1</b>	<b>3.16E-06</b>	<b>4.27E-02</b>	<b>9.61E-03</b>	<b>6.35E-03</b>	<b>8.47E-04</b>
<b>259502_at</b>	<b>At1g15670</b>	<b>Kelch repeat-containing F box family protein</b>	<b>1.1</b>	<b>1.05E-03</b>	<b>8.49E-03</b>	<b>2.29E-03</b>	<b>1.61E-08</b>	<b>2.68E-07</b>
<b>257206_at</b>	<b>At3g16530</b>	<b>Legume lectin family protein</b>	<b>1.1</b>	<b>5.18E-03</b>	<b>2.41E-01<sup>a</sup></b>	<b>4.41E-05</b>	<b>3.48E-02</b>	<b>9.58E-05</b>
260143_at	At1g71880	SUC1, member of sucrose-proton symporter family	1.1	5.87E-06	5.52E-16	8.17E-31	4.90E-11	1.90E-15
<b>250062_at</b>	<b>At5g17760</b>	<b>AAA-type ATPase family protein</b>	<b>1.0</b>	<b>6.62E-10</b>	<b>3.46E-05</b>	<b>1.71E-05</b>	<b>9.54E-05</b>	<b>5.02E-01<sup>a</sup></b>
259382_s_at	At3g16430	Acalin lectin family protein	1.0	1.06E-07	1.16E-01 <sup>a</sup>	3.06E-02	1.10E-03	9.92E-04
	At3g16420							
<b>259507_at</b>	<b>At1g43910</b>	<b>AAA-type ATPase family protein</b>	<b>1.0</b>	<b>5.90E-07</b>	<b>8.03E-12</b>	<b>8.07E-36</b>	<b>5.47E-11</b>	<b>1.14E-24</b>
<b>265067_at</b>	<b>At1g03850</b>	<b>Glutaredoxin family protein</b>	<b>1.0</b>	<b>2.62E-03</b>	<b>2.30E-03</b>	<b>1.88E-16</b>	<b>1.89E-01<sup>a</sup></b>	<b>2.13E-10</b>
265471_at	At2g37130	Peroxidase 21 (PER21, P21, PRXR5)	1.0	8.28E-03	3.97E-01 <sup>a</sup>	9.85E-02 <sup>a</sup>	2.02E-01 <sup>a</sup>	7.16E-01 <sup>a</sup>
252309_at	At3g49340	Cys proteinase, putative	1.0	2.34E-12	1.79E-09	4.07E-23	1.65E-13	1.19E-12
<b>252549_at</b>	<b>At3g45860</b>	<b>Receptor-like protein kinase</b>	<b>1.0</b>	<b>7.98E-06</b>	<b>7.33E-05</b>	<b>6.73E-20</b>	<b>2.58E-06</b>	<b>7.21E-11</b>
247109_at	At5g65870	Phytosulfokines 5 (PSK5)	1.0	3.03E-04	3.79E-09	1.34E-21	4.55E-10	3.87E-13
<b>246238_at</b>	<b>At4g36670</b>	<b>Mannitol transporter, putative</b>	<b>1.0</b>	<b>9.01E-03</b>	<b>4.28E-01<sup>a</sup></b>	<b>1.05E-02</b>	<b>1.33E-02</b>	<b>7.14E-01<sup>a</sup></b>
<b>256431_s_at</b>	<b>At3g11010</b>	<b>Disease resistance family protein, contains Leu-rich repeat domains</b>	<b>1.0</b>	<b>2.94E-02</b>	<b>5.84E-02<sup>a</sup></b>	<b>2.97E-15</b>	<b>1.15E-02</b>	<b>1.87E-13</b>
	At5g27060							
<b>255941_at</b>	<b>At1g20350</b>	<b>AtTIM17-1, mitochondrial inner membrane translocase</b>	<b>1.0</b>	<b>2.53E-19</b>	<b>1.89E-11</b>	<b>1.90E-18</b>	<b>3.41E-11</b>	<b>4.99E-08</b>
<b>249417_at</b>	<b>At5g39670</b>	<b>Calcium binding EF hand family protein</b>	<b>1.0</b>	<b>4.73E-05</b>	<b>6.60E-23</b>	<b>5.18E-41</b>	<b>1.95E-16</b>	<b>3.14E-21</b>
267181_at	At2g37760	Aldo/keto reductase family protein	1.0	2.54E-06	3.29E-01 <sup>a</sup>	1.39E-01 <sup>a</sup>	4.97E-02	1.23E-01 <sup>a</sup>
<b>264663_at</b>	<b>At1g09970</b>	<b>Leu-rich repeat transmembrane protein kinase</b>	<b>1.0</b>	<b>7.36E-05</b>	<b>8.98E-03</b>	<b>1.21E-01<sup>a</sup></b>	<b>9.33E-02<sup>a</sup></b>	<b>7.89E-04</b>

Genes that were upregulated in the BTH-treated wild type are shown in boldface, and genes that were downregulated in the BTH-treated wild type are shown in lightface.

<sup>a</sup>  $q \geq 0.05$ .

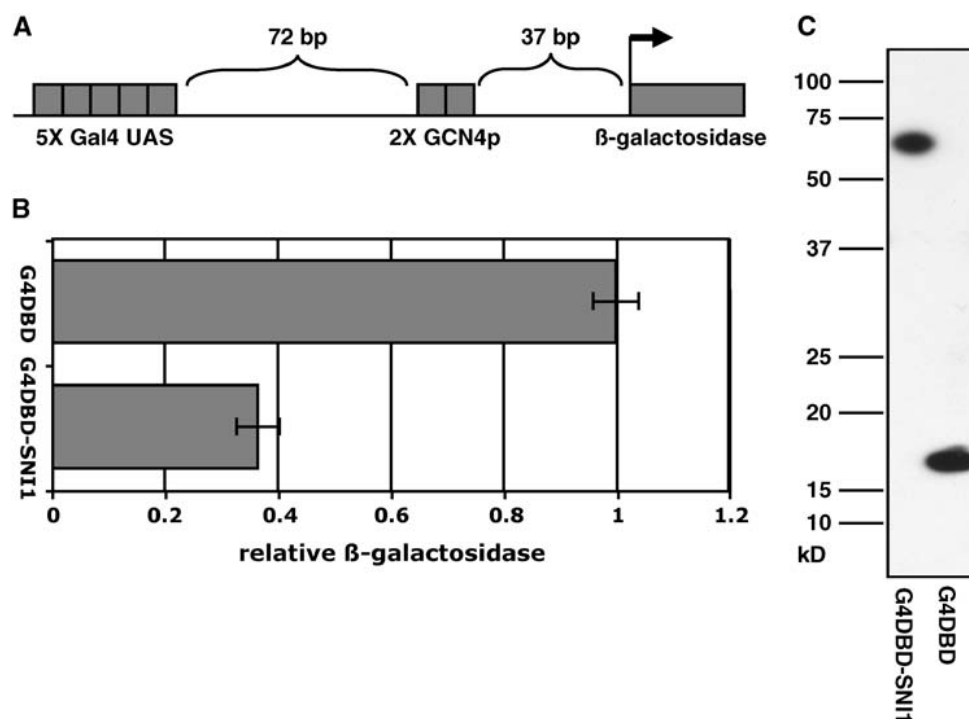


**Figure 2.** SNI1 Represses Transcription in a Yeast Expression System.

**(A)** The SS38 reporter gene.

**(B)** β-Galactosidase activity. SNI1 was fused to G4DBD in pMAN to generate G4DBD-SNI1 and transformed into yeast strain 122 carrying the integrated SS38 reporter gene. β-Galactosidase expression was measured using standard techniques (Sambrook and Russell, 2001). The values are given as averages  $\pm$  SE of three independent assays.

**(C)** Immunoblot with G4DBD and G4DBD-SNI1. Yeast protein extracts were run on an 8 to 18% gradient gel and probed with anti-G4DBD antibodies (Santa Cruz Biotechnology).

and lotus. Recently, full-length clones from tomato (*Solanum lycopersicum*) and rice were deposited in the NCBI database.

As shown in Figure 4A, the number and spacing of exons in *Os Sni1* and *Lj Sni1* are identical to those in *At SNI1*, indicating a conservation of genomic structure. To analyze the genomic structure of additional *SNI1* homologues, the genomic loci of *St Sni1* and *Gm Sni1* were cloned, sequenced, and aligned with cDNA sequences to identify introns. Interestingly, *St Sni1* and *Gm Sni1* share the same genomic structure as *At SNI1*, *Os Sni1*, and *Lj Sni1*.

To demonstrate the functionality of these putative *SNI1* orthologs, *St Sni1* and *Gm Sni1* were cloned behind *P<sub>35S</sub>* and transformed into *sni1* mutant plants. The ability of the transgenes to complement the *sni1-1* mutation was determined by the restoration of wild-type leaf morphology and the elimination of background expression of the *P<sub>BGL2</sub>::GUS* reporter gene. Among the 17 *P<sub>35S</sub>::Gm Sni1* transformants, 10 were found to partially or fully restore the wild-type phenotype, whereas 9 of 15 *P<sub>35S</sub>::St Sni1* transformants complement (Figure 4B). Additionally, *Gm Sni1* and *St Sni1* repress transcription in yeast (data not shown). These data demonstrate that *Gm Sni1* and *St Sni1* are true orthologs of *At SNI1*. Therefore, conserved functional domains in *SNI1* may be deduced through sequence alignment of these homologues.

Alignment of full-length *SNI1* homologues indicates that they are similar in length and that conservation exists throughout the

protein (Figure 5). Each homologue shares ~40% identity and 60% similarity with *At SNI1* and is ~10% longer than *At SNI1* because of insertions in three regions (Figure 5; see Supplemental Table 3 online). There are a number of residues that are perfectly conserved in all sequences, and in some instances these are present in blocks, for example, E/DV/ILDELxY and VRTR between residues 253 and 350 shown in Figure 5.

The homologues do not share sequence similarity with Rb, indicating that the similarity between *Arabidopsis SNI1* and Rb is unlikely to be functionally important. Iterative BLAST or BLAST of short, highly conserved regions yielded no proteins with similarity to *SNI1* other than the probable orthologs.

#### NAAIRS Mutagenesis Identifies Essential Residues in *SNI1*

To empirically determine which regions of the *SNI1* protein are essential for function, saturating mutagenesis of *At SNI1* was undertaken using the NAAIRS-scanning technique (Marsilio et al., 1991). The NAAIRS hexapeptide (Asp-Ala-Ala-Ile-Arg-Ser) naturally exists in multiple secondary structures (Wilson et al., 1985). In thermolysin, the NAAIRS peptide is found in a β-strand, whereas in phosphofructokinase, it is part of an α-helix (Evans and Hudson, 1979; Holmes and Matthews, 1982). It is believed that the NAAIRS peptide folds into a particular structure based upon the protein sequence context. Because of its flexible

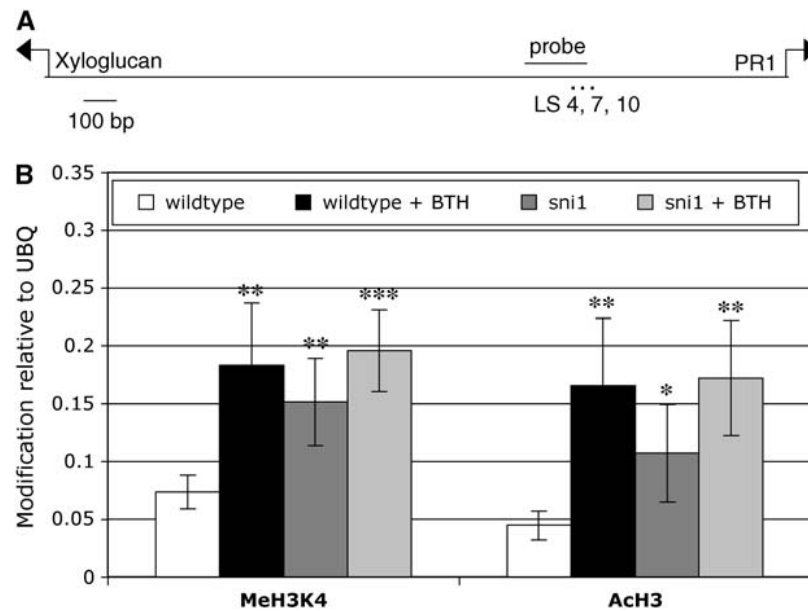


**Figure 3.** Chromatin Modifications at the *PR-1* Promoter.

**(A)** The *PR-1* promoter. Probe indicates the region amplified in chromatin immunoprecipitation experiments. LS 4, 7, and 10 are the promoter regions identified as important regulators of SAR induction (Lebel et al., 1998).

**(B)** Chromatin immunoprecipitation. Mean amount of *PR-1* promoter relative to ubiquitin associated with MeH3K4 and AcH3. Error bars indicate SE of four experiments, each in triplicate. Two-tailed *t* tests were performed on the data. The untreated wild type values are significantly lower than all other values for both modifications (\*  $P < 0.1$ , \*\*  $P < 0.05$ , \*\*\*  $P < 0.01$ ). None of the other samples are significantly different from each other.

nature, the NAAIRS peptide has been used for mutagenesis studies, replacing six amino acids at a time, with minimal disruption to the overall protein structure (Lonergan et al., 1998; Sellers et al., 1998; Armbruster et al., 2001; Banik et al., 2002).

Seventy-seven NAAIRS mutations were created to cover the entire SNI1 protein (Figure 5). Constructs were designed to mutate each residue at least once, with some substitutions being conservative. Because previous work showed that *P<sub>35S</sub>::SNI1* can complement the *sni1* mutation without any detectable ectopic expression effects (Li et al., 1999; X. Li and X. Dong, unpublished data), the NAAIRS mutant cDNAs were cloned behind *P<sub>35S</sub>*, sequenced, and transformed into the *sni1-1* background. For each construct, three independent transformants carrying single-locus insertions of the transgene (showing a 3:1 ratio of Basta resistance) were identified and carried to the T3 generation to identify homozygous lines for analysis. The functionality of each NAAIRS mutant was examined in planta by its ability to complement the phenotype conferred by *sni1*.

We chose root length as a measure of SNI1 function because it is quantitative and tightly correlated with other effects of SNI1, such as *P<sub>BGL2</sub>::GUS* reporter expression (see Supplemental Figure 1 online) and leaf morphology. For each transgenic line, ~15 seedlings were examined. Among the three independent lines for each NAAIRS construct, we noted a general consistency in root length and *P<sub>BGL2</sub>::GUS* reporter expression. We attribute any deviations observed among the independent lines to position effects or gene silencing. Many NAAIRS lines had intermediate root lengths, indicating that these mutations are hypomorphic. To categorize NAAIRS mutations into complementing and non-

complementing classes, a threshold value for root length was established. On average, the length of *sni1-1* roots is ~30% of the wild-type length, and >90% of the lines analyzed fell between 30 and 100% of the wild type in root length. Half of this difference (65%) was set as the arbitrary threshold for complementation. Those constructs with an average root length of at least one line above 65% of wild-type root length were regarded as complementing, whereas those uniformly (all three independent lines) below 65% were regarded as noncomplementary. The line with the longest average root length for each NAAIRS mutation is plotted in Figure 6. Regions essential for SNI1 function represented by the noncomplementing NAAIRS constructs occur throughout the protein, with the largest being from amino acids 24 to 73 and 278 to 313 (Figure 5; NAAIRS constructs 5 to 14 and 50 to 56, respectively). Consistently, these essential regions are highly conserved in the SNI1 homologues. On the other hand, regions with limited similarity (e.g., those represented by NAAIRS constructs 20, 41, and 69) were found to be nonessential for protein function. Interestingly, some regions of high conservation, such as NAAIRS mutations 47 to 49, are not essential for SNI1 function, indicating that they may play a regulatory role.

### 3D-PSSM Predictions Indicate That SNI1 Has Similarity to Armadillo Repeats

Because SNI1 shows no primary sequence homology with other proteins, we searched for structural homology in various databases. Prediction of protein structure is difficult and imprecise,



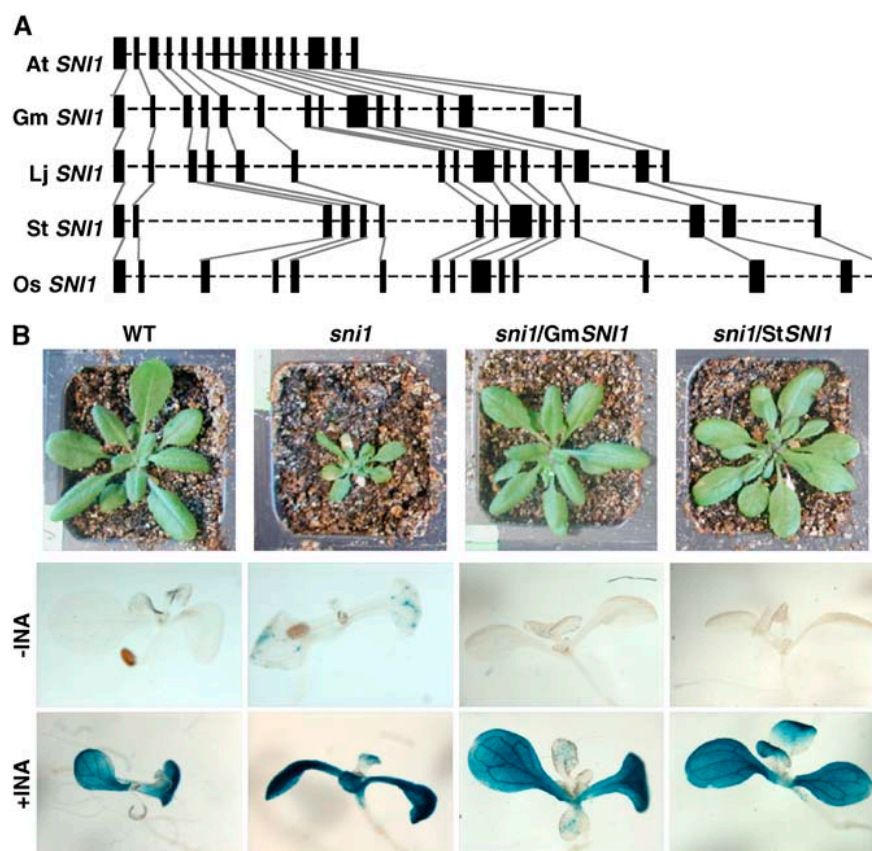


**Figure 4.** Structure and Function of SNI1 Are Conserved in Different Plant Species.

**(A)** Genomic structure of SNI1 homologues. At, *Arabidopsis*; Gm, soybean; Lj, lotus; St, potato; and Os, rice. The 15 exons of each locus are indicated with black boxes, introns are indicated by dashed lines, and corresponding exons in each plant species are connected by gray lines. All introns and exons are drawn to scale.

**(B)**  $P_{35S}::Gm\ SNI1$  and  $P_{35S}::St\ SNI1$  in the *sni1-1* background restore wild-type morphology and  $P_{BGL2}::GUS$  expression. Morphology was determined on 4-week-old, soil-grown plants.  $P_{BGL2}::GUS$  staining was conducted on seedlings grown for 12 d on MS plates with (+) or without (–) 10  $\mu$ M INA.

often yielding models with low certainty. However, comparison of homologous sequences can greatly support these predictions (Kretsinger et al., 2004). The three-dimensional position-specific scoring matrix (3D-PSSM) prediction program (<http://www.sbg.bio.ic.ac.uk/~3dpssm/>) creates a linear sequence of the predicted secondary structure of the query protein and compares it with the known patterns of secondary structures from solved protein structures (Kelley et al., 2000). It has been used successfully to reveal molecular functions of proteins such as JAR1 and AvrRpt2 (Staswick et al., 2002; Axtell et al., 2003).

At SNI1 and each of the full-length homologous sequences were subjected to 3D-PSSM analysis to find solved protein structures that might serve as templates. Of the template proteins identified,  $\alpha$ - $\alpha$  supercoil proteins were highly represented for each homologue, with Armadillo repeat (ARM) proteins most commonly represented. For At SNI1, Gm Sni1, St Sni1, and Lj Sni1, the template with the highest significance (lowest *E* value) was the ARM domain of *Mus musculus*  $\alpha$ -importin. 3D-PSSM confidence values range from 70 to 80% for each of these matches. For Lj Sni1, the best template structure was the ARM domain of *Homo sapiens*  $\beta$ -importin (90% confidence); *M. mus-*

*culus*  $\alpha$ -importin was second, with 80% certainty. Similarly, the best hit for So Sni1 was the ARM domain of *M. musculus*  $\beta$ -catenin (50% confidence). Only Os Sni1 failed to return an ARM protein with a confidence >50%. However, ARM proteins were highly represented among the less significant hits.

The At SNI1 sequence (amino acids 14 to 402) was threaded onto the ARM domain of *M. musculus*  $\alpha$ -importin (PDB structure 1ial) with the DeepView Swiss-Pdb viewer (Guex and Peitsch, 1997). The 3D-PSSM alignment (see Supplemental Figure 2 online) was adjusted manually to bridge gaps and reduce free energy and was submitted to SwissModel to create a protein structure file. Essential residues identified through NAAIRS mutagenesis were colored in DeepView to give an image of functionally important regions of the SNI1 protein (Figure 7).

ARM repeats form a superhelix of  $\alpha$ -helices that results in a spiral structure (Huber et al., 1997). In the case of  $\alpha$ -importin, the repeats create a twisted kidney bean shape (Conti et al., 1998). The two main functional regions in SNI1 identified through NAAIRS mutagenesis are localized near the N terminus and C terminus, at the two ends of the kidney bean. Interestingly, the smaller stretches of essential residues cluster on the concave

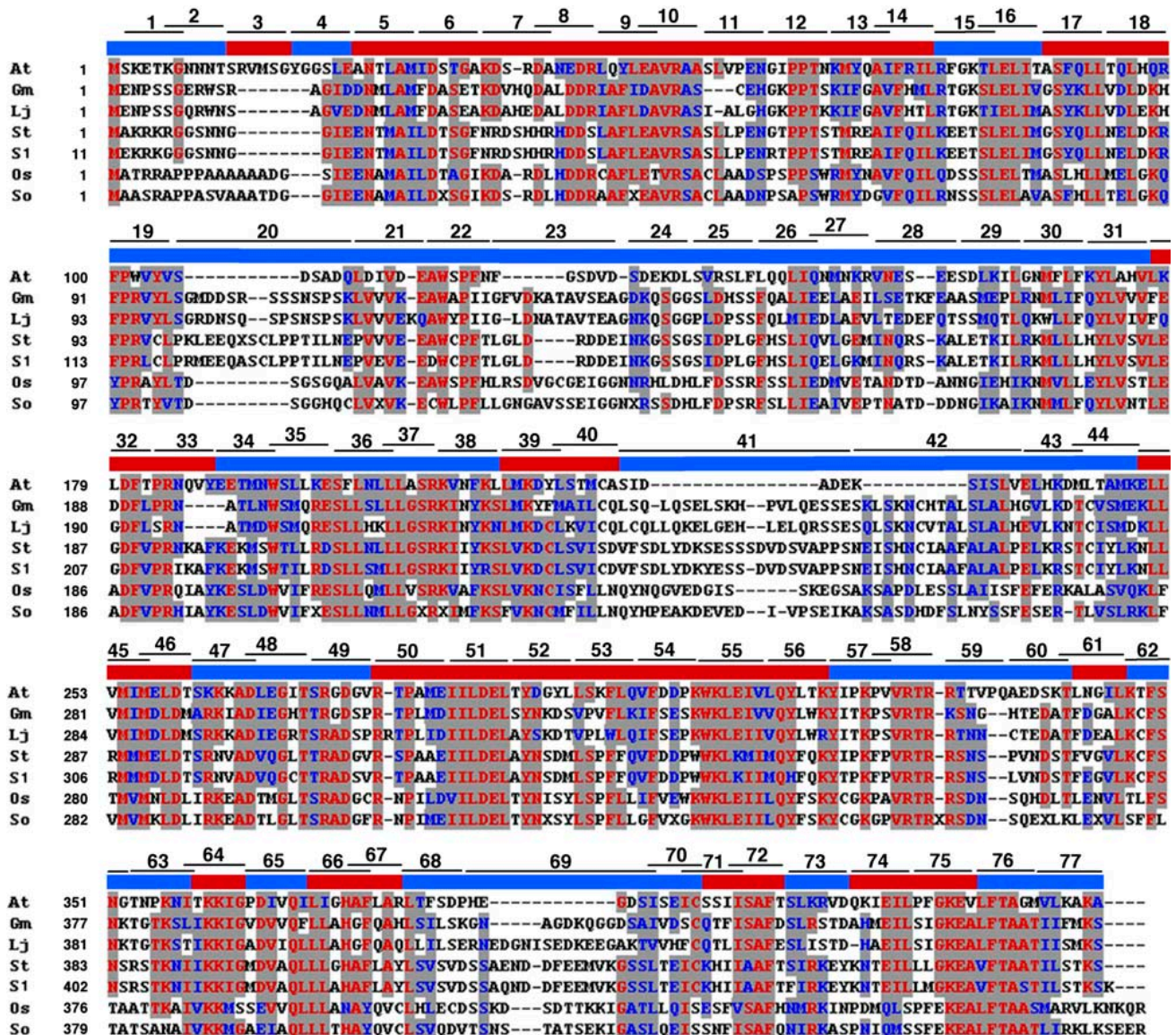


**Figure 5.** Sequence Conservation among the SNI1 Homologues and Outline of At SNI1 Functional Regions Identified by NAAIRS Mutagenesis.

Alignment of cloned and predicted full-length cDNAs from *Arabidopsis* (At), soybean (Gm), lotus (Lj), potato (St), tomato (Sl), rice (Os), and sugarcane (So). Highly conserved residues (>70% identity) are colored red, and moderately conserved residues (>70% similarity) are colored blue. The black numbered lines indicate residues in At SNI1 substituted by NAAIRS. The colored bars above the sequence alignment outline the functional regions of SNI1 defined by NAAIRS mutagenesis (see Figure 6): blue bars, regions nonessential for SNI1 activity; red bars, regions essential for SNI1 activity.

side of the structure, indicating the presence of a binding surface that was not apparent from the linear sequence.

## DISCUSSION

Although genetic evidence suggests that SNI1 is a transcriptional repressor (Li et al., 1999), its vanishingly low level of expression and lack of sequence homology with known proteins or domains have made the application of conventional biochemical and molecular methodologies ineffective. To remedy this, we developed a combination of genetic and genomic approaches to dissect the structure and function of this novel regulator.

The use of the GFP-SNI1 fusion protein allowed the observation of the subcellular localization of SNI1 in planta. Because of the extremely low protein levels and the background fluorescence of chlorophyll in green tissues, GFP-SNI1 fluorescence was visible only in roots. Although SAR is expressed only in the aerial parts of the plant, SNI1 is likely to be functional in roots because in the *sni1* mutant, root development is substantially impaired. The GFP-SNI1 fusion complemented all of the *sni1* phenotypes in both shoot and root tissues, indicating that the fusion protein is fully functional and accumulates in the proper subcellular location. Confocal imaging showed that GFP-SNI1



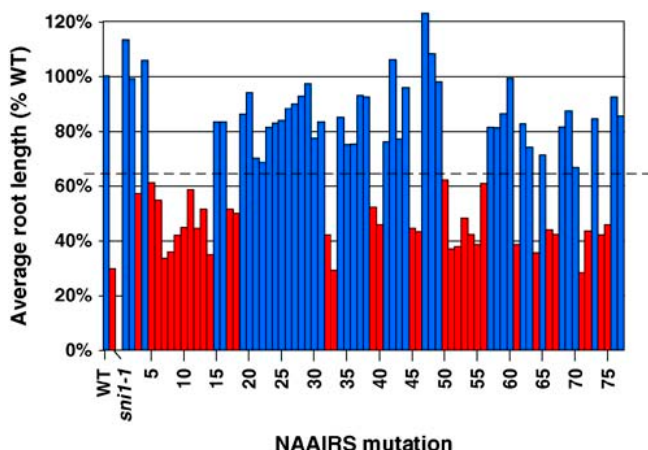


**Figure 6.** Functional Analysis of the NAAIRS Mutants.

Complementation of *sni1-1* by NAAIRS mutants as measured by root length. Approximately 15 homozygous NAAIRS mutants were grown vertically on MS plates for 8 d, and root length was measured. Colored bars represent average root length of the best complementing transgenic line for each NAAIRS mutant (number indicated on the x axis) compared with the wild type (set as 100%). The dashed line at 65% was set to separate the functional NAAIRS mutants (blue bars) from the nonfunctional NAAIRS mutants (red bars).

localizes primarily to the nucleus, consistent with transient expression in onion cells and the hypothesis that SNI1 is a transcriptional repressor.

Whole-genome transcription profiling data confirmed the inhibitory role of SNI1 in SAR-related gene transcription. In the *sni1* background, 23 times as many genes are upregulated (95 genes) as downregulated (4 genes). More importantly, 93 to 95% of the genes upregulated in *sni1* are BTH-responsive and NPR1-dependent in the wild type. This finding indicates a direct role for SNI1 in plant defense and supports the hypothesis that SNI1 functions downstream of NPR1.

The ability of SNI1 to repress transcription in yeast indicates that it functions through a highly conserved repression mechanism, such as histone modification, chromatin remodeling, or RNA polymerase II interference (Cowell, 1994; Gaston and Jayaraman, 2003). During the induction of SAR, changes are seen in the abundance of activating histone modifications, namely AcH3 and MeH3K4. These changes are mimicked in *sni1*, indicating that the loss of SNI1 function is sufficient to cause these chromatin modifications at the *PR-1* promoter. Intriguingly, SA is still required in *sni1* to fully induce *PR-1* and other SAR-related genes (Li et al., 1999). This finding indicates that there are still other SA-dependent regulators that function downstream of SNI1. Indeed, a genetic study showed that transcription in *sni1* requires the function of a protein known to be involved in chromatin remodeling (W.E. Durrant and X. Dong, unpublished data).

More study is required to determine the mechanism by which SNI1 modifies chromatin. It may inhibit the action of histone acetyltransferases or MeH3K4-specific methyltransferases, or it may counter those enzymes through histone deacetylation or H3K9-specific methylation. Because SNI1 has no homology with known chromatin modification enzymes, it likely serves as a

recruiter of inhibitory enzymes to promoters of defense-related genes. SNI1 may interact with only a single enzyme, which in turn recruits factors for complementary modifications, or with multiple enzymes carrying out different modifications.

Discovery of SNI1 orthologs in other plant species and genetic complementation of the *Arabidopsis sni1* mutation by Gm *Sni1* and St *Sni1* suggest that SNI1 function is highly conserved in the plant kingdom. In *Arabidopsis* and rice, for which the whole genome sequences are known, At *SNI1* and Os *Sni1* are single-copy genes. In addition, all of the ESTs that we have analyzed represent a single gene for the given species. Therefore, it is likely that there is only a single SNI1 ortholog in most plant species, which functions as a central regulator of plant defense.

Alignment of six full-length SNI1 homologues revealed regions of the protein with high sequence conservation. However, BLAST and TBLAST searches of protein databases with these highly conserved fragments have not yielded significant sequence similarities (low *E* values) with other proteins. Likewise, querying BLAST or TBLAST with sequences encoded by individual exons or with any fragment of At *SNI1* returns no similar proteins. Therefore, we conclude that SNI1 is a novel plant-specific protein. Interestingly, among the plant-specific proteins, transcriptional regulators are overrepresented (Gutierrez et al., 2004).

To identify functional domains of SNI1, we undertook a saturating mutagenesis of At *SNI1* using the NAAIRS-scanning technique (Marsilio et al., 1991). This technique has defined functional domains in the human telomerase (Armbruster et al., 2001; Banik et al., 2002) and von Hippel-Lindau tumor suppressor protein (Loneragan et al., 1998) and has separated the two functional regions within the pocket domain of Rb (Sellers et al., 1998).

The NAAIRS mutants of SNI1 (expressed in the *sni1-1* background) were characterized for their effects on defense gene expression and root development. As is the case for the endogenous *SNI1* and *P<sub>35S</sub>:SNI1*, RNA gel blot analysis showed that most NAAIRS mutants were expressed at undetectable levels in planta. However, immunoblot analysis of the NAAIRS mutants expressed in yeast showed that the mutations had no effect on SNI1 protein stability (see Supplemental Figure 3 online). Additionally, nearly all NAAIRS mutations had a less severe phenotype than the *sni1-1* allele, indicating that they are not null

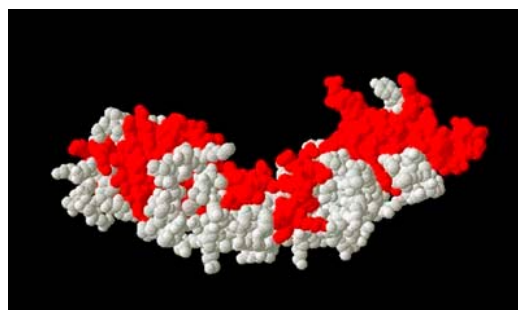


**Figure 7.** Modeling of the SNI1 Protein.

At *SNI1* (amino acids 14 to 402) was threaded onto the ARMs of  $\alpha$ -importin (*M. musculus*; amino acids 70 to 496). Residues identified as essential via NAAIRS mutagenesis are colored red.

mutations. From this, we conclude that the phenotypes of NAAIRS transgenic lines are attributable to the specific mutation of six residues of SNI1 and likely not to the disruption of protein expression or stability. Among the NAAIRS transgenic lines, we noticed an inverse correlation between the levels of defense gene expression (as measured by the *P<sub>BGL2</sub>:GUS* reporter) and root length, supporting the hypothesis that the morphology of *sn1* is a consequence of unregulated defense gene expression. To eliminate abrogating factors such as position effects or silencing of the transgene, the functionality of each NAAIRS mutant was determined using the best complementing line (longest average root length) among the three independent transformants. NAAIRS mutagenesis identified two large regions (amino acids 24 to 73 and 278 to 313) and several smaller regions in SNI1 that are essential for activity in planta. These essential regions are highly conserved among the SNI1 homologues.

Multiple predictions of secondary structure for SNI1 and its homologues indicate that they are primarily  $\alpha$ -helical in nature. Using the 3D-PSSM software, a linear prediction of secondary structure was compared against the known sequences of secondary structures from solved proteins. It was determined that At SNI1 and each of the full-length homologous sequences have high structural similarity to  $\alpha$ - $\alpha$  supercoil proteins, specifically ARMs.

ARMs exist in many different types of proteins and are best characterized in the transcriptional regulator Armadillo/ $\beta$ -catenin and the nuclear import regulators  $\alpha$ - and  $\beta$ -importin (Coates, 2003). Each 42-amino acid repeat forms three  $\alpha$ -helices, which stack with other repeats in a superhelix. In ARM repeats, this superhelix has an additional level of spiral, creating one convex and one concave surface. It is hypothesized that  $\alpha$ - $\alpha$  supercoil domains (including the ARM) serve to create a large surface area for protein-protein interactions (Groves and Barford, 1999). In particular, the concave inner surfaces of Armadillo/ $\beta$ -catenin and  $\alpha$ -importin are the binding sites of cadherins and basic nuclear localization signals, respectively (Conti et al., 1998; Willert and Nusse, 1998; Huber and Weis, 2001). The ARM repeats of  $\beta$ -catenin are also involved in transcriptional regulation by binding transcription factors such as LEF and TCF in the nucleus (Willert and Nusse, 1998).

SNI1 and its homologues do not share sequence similarity with  $\alpha$ -importin,  $\beta$ -catenin, or other ARM proteins. However, 3D-PSSM predictions indicate that they have a similar  $\alpha$ - $\alpha$  superhelical shape. To map the essential SNI1 residues in three-dimensional space, the At SNI1 sequence was threaded onto the ARM repeats of  $\alpha$ -importin. Interestingly, most of the essential regions identified through NAAIRS mutagenesis fall within the concave surface of the threaded structure. Because SNI1 does not appear to have a DNA binding domain, it is possible that this interaction surface binds a transcription factor, such as a WRKY factor, to localize SNI1 to the *PR* promoters. This surface could also bind a chromatin-modifying enzyme to cause transcriptional repression. Constitutive nuclear localization of the GFP-SNI1 fusion indicates that subcellular localization is unlikely to be a mechanism that regulates SNI1 activity. However, because GFP-SNI1 was observed only in the root tissue, we cannot rule out this possibility for leaf cells. Although no change in the intensity of GFP-SNI1 was observed before and after INA induction, more experimentation is required to determine whether protein degradation is involved in the removal of SNI1 repression. Gel

mobility variations observed for some of the NAAIRS mutant proteins expressed in yeast (data not shown) suggest that SNI1 is probably posttranslationally modified and that such modification may influence its activity. Preliminary results also indicate that some complementing NAAIRS mutants are less sensitive to INA induction, as measured by *P<sub>BGL2</sub>:GUS* reporter expression (data not shown). These mutations coincide with regions of conservation among the homologues, further supporting the hypothesis of a conserved regulatory region in this protein. Curiously, none of these NAAIRS mutants completely abolished the protein's responsiveness to SAR induction.

Compared with transcriptional activators, much less is known about transcriptional repressors. This is especially true in plants. Through this study, we give evidence to indicate that SNI1 is a nucleus-localized transcriptional repressor functioning through a highly conserved active repression mechanism. Even though SNI1 appears to be a plant-specific protein based on its primary sequence, its structural similarity to ARM proteins indicates that there may be other proteins with similarity to SNI1 that are divergent at the level of primary sequence. In a recent report, the SYS-1 protein of *Caenorhabditis elegans* was shown to function as a  $\beta$ -catenin in its transcriptional cofactor activity (Kidd et al., 2005). This extremely weakly expressed protein does not have significant sequence similarity to  $\beta$ -catenin but has a level of structural similarity to  $\beta$ -catenin (analyzed by 3D-PSSM) comparable to that of SNI1.

## METHODS

### Cloning, Transformation, and Plant Growth Conditions

Cloning and bacterial and yeast transformation followed standard molecular biology protocols (Sambrook and Russell, 2001). To ensure that no unintended mutations occurred during PCR, a 20:1 Taq:Pfu mixture was used and all constructs were sequenced (BigDye; Applied Biosystems) before transformation. *Arabidopsis thaliana* transformation was via the floral dip method (Bent, 2000) using *Agrobacterium tumefaciens* strain GV3101 (Hellens et al., 2000). Plants were grown in MetroMix 200 (Scotts) under standard conditions (Weigel and Glazebrook, 2002). Binary constructs used in this work were made using the pRAM vector containing the Basta resistance gene (*bar*; see Supplemental Figure 4 online; Xiang et al., 1999). All transgenic lines and mutants are in the Columbia ecotype and contain the *P<sub>BGL2</sub>:GUS* reporter. For the yeast transcription repression assay, the pMAN vector was generated by adding new *Bam*HI and *Sac*I sites in frame with G4DBD into the vector pMA424 (Ma and Ptashne, 1987) for easy cloning from pRAM.

Basta selection of primary transformants was conducted on soil. One-week-old seedlings were sprayed with a 1:500 dilution of Finale (Bayer CropScience). When necessary, additional spraying was performed until the entire flat was exposed to the herbicide. Resistant plants (T1) were transplanted to fresh soil and grown to maturity. To determine the segregation of Basta resistance, seedlings were grown for 1 week on Murashige and Skoog (MS) medium (Caisson Laboratories) with vitamins (Sigma-Aldrich) and 50  $\mu$ M Basta (glufosinate ammonium; Crescent Chemical). Susceptible and resistant seedlings were counted and subjected to  $\chi^2$  analysis for 3:1 segregation of a single-locus insertion. Only lines with a  $\chi^2$  value < 1.5 were characterized further.

All root length measurements are averages of triplicates of  $\sim$ 15 seedlings grown vertically on MS medium with vitamins for 8 d. Soil-grown plants were grown as described previously (Cao et al., 1994).

### Confocal Microscopy

The *P<sub>35S</sub>:GFP-SNI1* transgenic lines were grown on vertically placed MS (1% sucrose) plates for 5 d. Roots were treated for 1 to 2 min in 10  $\mu$ g/mL propidium iodide to stain cell walls before microscopy. A  $\times 60$  water-immersion lens and a 488-nm laser were used with a Zeiss LSM-510 laser-scanning confocal microscope. GFP fluorescence was false-colored green and propidium iodide was false-colored red.

### Microarray Analysis

To identify genes affected by the *sn1* mutation, RNA was extracted from 4-week-old, soil-grown, untreated wild-type and *sn1* plants. Equal amounts of three independent RNA samples were pooled for each genotype. Probes were made from the RNA samples and hybridized to the Affymetrix *Arabidopsis* ATH1 GeneChip arrays (Redman et al., 2004) according to the manufacturer's protocol. Hybridizations were performed by the Duke Microarray Core Facility at the Center for Applied Genomics and Technology (Duke University). Three independent experiments were performed, and the data were analyzed using a mixed-model ANOVA described by Levesque et al. (2006). Briefly, probe-level signals were globally normalized and  $\log_2$ -transformed, with their means centered to zero for each array. Next, a mixed-model ANOVA was applied based on that developed by Chu et al. (2004). In this analysis, the output of the global normalization procedure for each gene is attributed to genotype, probe, and array effects as well as a standard error term. From this model, the mean expression value and a raw P value for the probability of falsely rejecting the null hypothesis of no differential expression for every gene were calculated. Finally, multiple testing correction for type I family-wise error was performed using the method proposed by Storey and Tibshirani (2003). Genes that showed significant differences ( $q$  value  $< 0.05$ ) in expression between the wild type and *sn1* in all three experiments were identified first. A twofold cutoff was then applied to further narrow the list of genes. To identify genes regulated by BTH and NPR1, 4-week-old, soil-grown wild-type and *npr1-1* plants were treated with 60  $\mu$ M BTH for 0, 8, and 24 h before collection. RNA samples were prepared, pooled, and hybridized as described above. Three independent biological replicates were made for both the wild type and *npr1-1* for all three time points. To identify the BTH-responsive genes, wild-type samples at 8 and 24 h after treatment were compared with 0-h samples using mixed-model ANOVA with multiple testing correction for type I family-wise error. Those genes with  $q$  values  $< 0.05$  at either time point were considered BTH-responsive. To identify NPR1-dependent genes, *npr1-1* samples at 8 and 24 h after BTH treatment were compared with those in the wild type. The same statistical tools were applied. Genes that were differentially expressed in *npr1-1* compared with the wild type ( $q$  value  $< 0.05$ ) at either time point were considered NPR1-dependent.

To identify functional classes of genes among those expressed more highly in *sn1* than in the wild type, we used DAVID 2.1 (Dennis et al., 2003; <http://david.abcc.ncifcrf.gov/>) to analyze gene ontology terms for biological processes. DAVID 2.1 allowed us to identify functional classes that are significantly overrepresented compared with the *Arabidopsis* genome as a whole using the Fisher exact test for enrichment analysis.

### Yeast Transcription Repression Assay

The wild-type SNI1 cDNA and the NAAIRS mutants were excised from the pRAM vector and cloned into the *Bam*HI and *Sac*I sites of the pMAN vector. The constructs were transformed into yeast strain 122 carrying the SS38 reporter gene (Saha et al., 1993). Yeast cells harboring the indicated plasmids were cultivated overnight in synthetically defined medium (Ura<sup>-</sup> and His<sup>-</sup>), transferred to fresh medium, and grown to OD<sub>600</sub> between 0.5 and 1.0.  $\beta$ -Galactosidase activity of the cell extract was measured using standard techniques (Sambrook and Russell, 2001). The values are averages and standard errors of three independent assays.

### Chromatin Immunoprecipitation

Chromatin immunoprecipitation was performed using a method modified from Johnson et al. (2002). Two to 3 g of 4-week-old, soil-grown plants ( $\sim 100$  wild type or 200 *sn1*) were untreated or sprayed with 300  $\mu$ M BTH (Novartis). Forty-eight hours later, tissue was collected and infiltrated with buffer A (400 mM sucrose, 10 mM Tris, pH 8, 1 mM EDTA, 1 mM phenylmethylsulfonyl fluoride, and 1% formaldehyde). Tissue was cross-linked for 10 min before the addition of Gly to a final concentration of 100 mM, washed in distilled water, and homogenized in 5 mL of cold lysis buffer (50 mM HEPES, pH 7.5, 150 mM NaCl, 0.5% Triton X-100, 1 mM phenylmethylsulfonyl fluoride, 10 mM sodium butyrate, and a 1:100 dilution of plant protease inhibitor cocktail; Sigma-Aldrich). Lysate was sonicated two times for 1 min each (amplitude, 21%) on a Branson digital sonicator, and debris was pelleted by centrifugation. Chromatin solution was cleared with single-stranded DNA/protein A beads (Upstate) at 4°C for 3 h with rotation. Fifty microliters of the resulting solution was taken as an input sample, and 500  $\mu$ L was used for each immunoprecipitation sample. Immunoprecipitation samples were incubated with 10  $\mu$ L of anti-MeH3K4 antibody (Upstate; 07-030), 10  $\mu$ L of anti-AcH3 antibody (Upstate; 06-599), or no antibody overnight with rotation at 4°C. To collect chromatin fragments, 30  $\mu$ L of single-stranded DNA/protein A beads (Upstate) was added to each immunoprecipitation sample and incubated with rotation for an additional 3 h. Beads were pelleted and washed with 500  $\mu$ L per wash. Five washes were conducted: one low-salt wash (150 mM NaCl, 0.2% SDS, 0.5% Triton X-100, 2 mM EDTA, and 20 mM Tris, pH 8); one high-salt wash (500 mM NaCl, 0.2% SDS, 0.5% Triton X-100, 2 mM EDTA, and 20 mM Tris, pH 8); one lithium chloride wash (0.25 M LiCl, 0.5% Nonidet P-40, 0.5% sodium deoxycholate, 1 mM EDTA, and 10 mM Tris, pH 8); and two TE washes (10 mM Tris, pH 7.5, and 1 mM EDTA). Chromatin fragments were eluted by incubation with 250  $\mu$ L of fresh elution buffer (1% SDS and 100 mM NaHCO<sub>3</sub>) at 65°C for 15 min with agitation. Elution was repeated, and the two eluates were combined. Elution buffer (450  $\mu$ L) was added to the 50- $\mu$ L input sample, and this was included with immunoprecipitation samples. To reverse cross-linking, 20  $\mu$ L of 5 M NaCl was added and each sample was incubated overnight at 65°C.

Samples were treated with RNase for 10 min at room temperature before proteinase K digestion. Ten microliters of 0.5 M EDTA, 20  $\mu$ L of 1 M Tris, pH 6.8, and 20  $\mu$ g of proteinase K were added, and samples were incubated for 1 h at 45°C. DNA was purified by phenol/chloroform extraction, precipitated with 1  $\mu$ L of glycogen (15  $\mu$ g/ $\mu$ L), 50  $\mu$ L of 3 M sodium acetate, and 1 mL of ethanol, and resuspended in 50  $\mu$ L of sterile water. Input samples were further diluted 10-fold.

Quantitative PCR was performed in a LightCycler (Roche) with Quantitect SYBR Green Master Mix (Qiagen). Half-size reactions were performed as recommended by Qiagen with the exception that reactions to amplify the *PR-1* promoter were supplemented with MgCl<sub>2</sub> to a final concentration of 4  $\mu$ M. All primers were designed by LightCycler Probe Design Software (Roche): UBQ5, 5'-GACGCTTCATCTCGTCC-3' and 5'-GTAACGTTAGGTGAGTCCA-3'; *PR-1* promoter, 5'-CGCCACATCT-ATGACG-3' and 5'-GATCGGTCACCTAGAGT-3'. The amount of each target was equal to 2<sup>-C<sub>p</sub></sup>, where C<sub>p</sub> is the crossing point as determined by second derivative maximum (LightCycler software). The success of each immunoprecipitation was determined by comparing the amount of UBQ5 relative to the amount in the no-antibody control. Relative modification for each immunoprecipitation (IP) was determined with the following formula:

$$= \frac{\text{amount PR-1 promoter (IP)}/\text{amount UBQ5 (IP)}}{\text{amount PR-1 promoter (input)}/\text{amount UBQ5 (input)}}$$

Each immunoprecipitation was conducted in triplicate and the experiment performed four times.

### Cloning of SNI1 Orthologs

RNA was extracted from young soybean (*Glycine max*) or potato (*Solanum tuberosum*) leaves using RNAqueous columns and Plant RNA Isolation Aid (Ambion) as recommended by the manufacturer. After quantification, mRNA was purified from 10  $\mu$ g of total RNA using Dynabeads oligo(dT)<sub>25</sub> (Dyna) and eluted in 10  $\mu$ L according to the manufacturer's instructions. Half of the purified mRNA was used for RNA ligase-mediated rapid amplification of cDNA ends using the GeneRacer kit (Invitrogen). Touchdown PCR was first conducted with primers to an EST and either the 5' or 3' adapter. The PCR product was then used as a template for nested PCR using nested primers at either or both ends. The final PCR products were cloned and sequenced.

Putative exons of the soybean and potato *SNI1* genes were predicted based on the genomic structure of the *Arabidopsis SNI1* gene, and primers were designed for each exon. Genomic DNA was isolated from soybean and potato leaf tissues using standard cetyl-trimethyl-ammonium bromide preparation (Weigel and Glazebrook, 2002) and used for PCR of the *SNI1* loci. PCR products were cloned and sequenced. Introns were determined by alignment of genomic and cDNA sequences.

Homologous protein sequences were aligned using ClustalW (Thompson et al., 1994) and visualized with BioEdit (Altschul et al., 1990; Hall, 1999). Pairwise comparisons were conducted using BLASTP (Altschul et al., 1990).

### Construction of NAAIRS Mutations

NAAIRS constructs were designed to substitute every amino acid in SNI1 except the first Met. The pRAM vector containing *P<sub>35S</sub>:SNI1* was used as a template. To make each NAAIRS construct, sequences upstream and downstream of the region of substitution were amplified separately using primers that introduce the NAAIRS coding sequence 3' and 5' of the resulting PCR fragments, respectively. One microliter of each of the fragments, which overlap in the NAAIRS coding region, was then mixed and used as a template for a third PCR using primers to the start and stop of the SNI1 cDNA. The resulting full-length cDNA containing the NAAIRS substitution was then excised from an agarose gel and cloned using standard techniques. For all mutations, the NAAIRS peptide was coded by the oligonucleotide 5'-AATGCTGCTATACGATCG-3'.

### Accession Numbers

Microarray data have been deposited in the Integrated Microarray Database System (<http://ausubellab.mgh.harvard.edu/imds/>) and NASC-Arrays (<http://affymetrix.Arabidopsis.info/donating.html>). Gm *SNI1* and St *SNI1* genomic and cDNA sequences have been deposited in GenBank with accession numbers DQ473313, DQ473314, DQ468343, and DQ468344.

### Supplemental Data

The following materials are available in the online version of this article.

**Supplemental Table 1.** Gene Ontology Terms Significantly Overrepresented among the Genes Expressed More Highly in *sni1* Than in the Wild Type.

**Supplemental Table 2.** ESTs with Similarity to SNI1.

**Supplemental Table 3.** Pairwise BLAST of SNI1 Homologues.

**Supplemental Figure 1.** Correlation between Average Root Length and Average Background *P<sub>BG2</sub>:GUS* Expression for all NAAIRS Mutants.

**Supplemental Figure 2.** Alignment of *Arabidopsis SNI1* (Amino Acids 14 to 402) and the ARMs of *M. musculus*  $\alpha$ -Importin (Amino Acids 70 to 496).

**Supplemental Figure 3.** Representative NAAIRS Constructs as G4DBD Fusions in Yeast.

**Supplemental Figure 4.** Map of pRAM.

### ACKNOWLEDGMENTS

We thank Kimberly Gallagher for helping with confocal microscopy, Zhongchi Liu for providing the yeast expression system, Christopher Counter for suggestions on NAAIRS mutagenesis, Nicolas Guex and Yigong Shi for advice on SNI1 modeling, Siobhan Brady and Natalie Weaver for advice on microarray analysis, Jason Bell for statistical advice, and Philip Benfey, Zhen-Ming Pei, and James Siedow for critiquing the manuscript. This work was supported by a graduate research fellowship from the National Science Foundation to R.A.M., a postdoctoral fellowship from the International Human Frontier Science Program Organization to W.E.D., and grants from the National Science Foundation (MCB-0090887 and MCB-0114783) to X.D.

Received November 23, 2005; revised April 29, 2006; accepted May 11, 2006; published June 9, 2006.

### REFERENCES

- Altschul, S.F., Gish, W., Miller, W., Myers, E.W., and Lipman, D.J. (1990). Basic local alignment search tool. *J. Mol. Biol.* **215**, 403–410.
- Altschul, S.F., Madden, T.L., Schaffer, A.A., Zhang, J., Zhang, Z., Miller, W., and Lipman, D.J. (1997). Gapped BLAST and PSI-BLAST: A new generation of protein database search programs. *Nucleic Acids Res.* **25**, 3389–3402.
- Armbruster, B.N., Banik, S.S., Guo, C., Smith, A.C., and Counter, C.M. (2001). N-terminal domains of the human telomerase catalytic subunit required for enzyme activity in vivo. *Mol. Cell. Biol.* **21**, 7775–7786.
- Axtell, M.J., Chisholm, S.T., Dahlbeck, D., and Staskawicz, B.J. (2003). Genetic and molecular evidence that the *Pseudomonas syringae* type III effector protein AvrRpt2 is a cysteine protease. *Mol. Microbiol.* **49**, 1537–1546.
- Banik, S.S., Guo, C., Smith, A.C., Margolis, S.S., Richardson, D.A., Tirado, C.A., and Counter, C.M. (2002). C-terminal regions of the human telomerase catalytic subunit essential for in vivo enzyme activity. *Mol. Cell. Biol.* **22**, 6234–6246.
- Bent, A.F. (2000). *Arabidopsis* in planta transformation. Uses, mechanisms, and prospects for transformation of other species. *Plant Physiol.* **124**, 1540–1547.
- Bowling, S.A., Clarke, J.D., Liu, Y., Klessig, D.F., and Dong, X. (1997). The *cpr5* mutant of *Arabidopsis* expresses both NPR1-dependent and NPR1-independent resistance. *Plant Cell* **9**, 1573–1584.
- Bowling, S.A., Guo, A., Cao, H., Gordon, A.S., Klessig, D.F., and Dong, X. (1994). A mutation in *Arabidopsis* that leads to constitutive expression of systemic acquired resistance. *Plant Cell* **6**, 1845–1857.
- Brogli, K., Chet, I., Holliday, M., Cressman, R., Biddle, P., Knowlton, S., Mauvais, C.J., and Brogli, R. (1991). Transgenic plants with enhanced resistance to the fungal pathogen *Rhizoctonia solani*. *Science* **254**, 1194–1197.
- Cao, H., Bowling, S.A., Gordon, S., and Dong, X. (1994). Characterization of an *Arabidopsis* mutant that is nonresponsive to inducers of systemic acquired resistance. *Plant Cell* **6**, 1583–1592.
- Chu, T.M., Weir, B.S., and Wolfinger, R.D. (2004). Comparison of Li-Wong and loglinear mixed models for the statistical analysis of oligonucleotide arrays. *Bioinformatics* **20**, 500–506.
- Clarke, J.D., Aarts, N., Feys, B.J., Dong, X., and Parker, J.E. (2001). Constitutive disease resistance requires *EDS1* in the *Arabidopsis*

- mutants *cpr1* and *cpr6* and is partially *EDS1*-dependent in *cpr5*. *Plant J.* **26**, 409–420.
- Clarke, J.D., Liu, Y., Klüssig, D.F., and Dong, X. (1998). Uncoupling PR gene expression from NPR1 and bacterial resistance: Characterization of the dominant *Arabidopsis cpr6-1* mutant. *Plant Cell* **10**, 557–569.
- Clarke, J.D., Volko, S.M., Ledford, H., Ausubel, F.M., and Dong, X. (2000). Roles of salicylic acid, jasmonic acid, and ethylene in *cpr*-induced resistance in *Arabidopsis*. *Plant Cell* **12**, 2175–2190.
- Coates, J.C. (2003). Armadillo repeat proteins: Beyond the animal kingdom. *Trends Cell Biol.* **13**, 463–471.
- Conti, E., Uy, M., Leighton, L., Blobel, G., and Kuriyan, J. (1998). Crystallographic analysis of the recognition of a nuclear localization signal by the nuclear import factor karyopherin alpha. *Cell* **94**, 193–204.
- Cowell, I.G. (1994). Repression versus activation in the control of gene transcription. *Trends Biochem. Sci.* **19**, 38–42.
- Delaney, T.P., Friedrich, L., and Ryals, J.A. (1995). *Arabidopsis* signal transduction mutant defective in chemically and biologically induced disease resistance. *Proc. Natl. Acad. Sci. USA* **92**, 6602–6606.
- Dennis, G., Jr., Sherman, B.T., Hosack, D.A., Yang, J., Gao, W., Lane, H.C., and Lempicki, R.A. (2003). DAVID: Database for Annotation, Visualization, and Integrated Discovery. *Genome Biol.* **4**, P3.
- Després, C., DeLong, C., Glaze, S., Liu, E., and Fobert, P.R. (2000). The *Arabidopsis* NPR1/NIM1 protein enhances the DNA binding activity of a subgroup of the TGA family of bZIP transcription factors. *Plant Cell* **12**, 279–290.
- Durrant, W.E., and Dong, X. (2004). Systemic acquired resistance. *Annu. Rev. Phytopathol.* **42**, 185–209.
- Evans, P.R., and Hudson, P.J. (1979). Structure and control of phosphofructokinase from *Bacillus stearothermophilus*. *Nature* **279**, 500–504.
- Gaston, K., and Jayaraman, P.S. (2003). Transcriptional repression in eukaryotes: Repressors and repression mechanisms. *Cell. Mol. Life Sci.* **60**, 721–741.
- Groves, M.R., and Barford, D. (1999). Topological characteristics of helical repeat proteins. *Curr. Opin. Struct. Biol.* **9**, 383–389.
- Guex, N., and Peitsch, M.C. (1997). SWISS-MODEL and the Swiss-PdbViewer: An environment for comparative protein modeling. *Electrophoresis* **18**, 2714–2723.
- Gutierrez, R.A., Green, P.J., Keegstra, K., and Ohlrogge, J.B. (2004). Phylogenetic profiling of the *Arabidopsis thaliana* proteome: What proteins distinguish plants from other organisms? *Genome Biol.* **5**, R53.
- Hall, T.A. (1999). BioEdit: An user friendly biological sequence alignment editor and analysis program for Windows 95/98/NT. *Nucl. Acids Symp. Ser.* **41**, 95–98.
- Heidel, A.J., Clarke, J.D., Antonovics, J., and Dong, X. (2004). Fitness costs of mutations affecting the systemic acquired resistance pathway in *Arabidopsis thaliana*. *Genetics* **168**, 2197–2206.
- Heil, M., Hilpert, A., Kaiser, W., and Linsenmair, K.E. (2000). Reduced growth and seed set following chemical induction of pathogen defence: Does systemic acquired resistance (SAR) incur allocation costs? *J. Ecol.* **88**, 645–654.
- Hellens, R., Mullineaux, P., and Klee, H. (2000). Technical Focus. A guide to Agrobacterium binary Ti vectors. *Trends Plant Sci.* **5**, 446–451.
- Holmes, M.A., and Matthews, B.W. (1982). Structure of thermolysin refined at 1.6 Å resolution. *J. Mol. Biol.* **160**, 623–639.
- Huber, A.H., Nelson, W.J., and Weis, W.I. (1997). Three-dimensional structure of the armadillo repeat region of beta-catenin. *Cell* **90**, 871–882.
- Huber, A.H., and Weis, W.I. (2001). The structure of the beta-catenin/E-cadherin complex and the molecular basis of diverse ligand recognition by beta-catenin. *Cell* **105**, 391–402.
- Hunt, M.D., Delaney, T.P., Dietrich, R.A., Weyman, K.B., Dangl, J.L., and Ryals, J.A. (1997). Salicylate-independent lesion formation in *Arabidopsis lsd* mutants. *Mol. Plant Microbe Interact.* **10**, 531–536.
- Johnson, L., Cao, X., and Jacobsen, S. (2002). Interplay between two epigenetic marks. DNA methylation and histone H3 lysine 9 methylation. *Curr. Biol.* **12**, 1360–1367.
- Kelley, L.A., MacCallum, R.M., and Sternberg, M.J. (2000). Enhanced genome annotation using structural profiles in the program 3D-PSSM. *J. Mol. Biol.* **299**, 499–520.
- Kidd, A.R., Miskowski, J.A., Siegfried, K.R., Sawa, H., and Kimble, J. (2005). A beta-catenin identified by functional rather than sequence criteria and its role in Wnt/MAPK signaling. *Cell* **121**, 761–772.
- Kretsinger, R.H., Ison, R.E., and Hovmoller, S. (2004). Prediction of protein structure. *Methods Enzymol.* **383**, 1–27.
- Lebel, E., Heifetz, P., Thorne, L., Uknes, S., Ryals, J., and Ward, E. (1998). Functional analysis of regulatory sequences controlling PR-1 gene expression in *Arabidopsis*. *Plant J.* **16**, 223–233.
- Levesque, M.P., Vernoux, T., Busch, W., Cui, H., Wang, J.Y., Bilou, I., Hassan, H., Nakajima, K., Matsumoto, N., Lohmann, J.U., Scheres, B., and Benfey, P.N. (2006). Whole-genome analysis of the SHORT-ROOT developmental pathway in *Arabidopsis*. *PLoS Biol.* **4**, 739–752.
- Li, X., Zhang, Y., Clarke, J.D., Li, Y., and Dong, X. (1999). Identification and cloning of a negative regulator of systemic acquired resistance, SN11, through a screen for suppressors of *npr1-1*. *Cell* **98**, 329–339.
- Liu, D., Raghothama, K.G., Hasegawa, P.M., and Bressan, R.A. (1994). Osmotin overexpression in potato delays development of disease symptoms. *Proc. Natl. Acad. Sci. USA* **91**, 1888–1892.
- Loneragan, K.M., Iliopoulos, O., Ohh, M., Kamura, T., Conaway, R.C., Conaway, J.W., and Kaelin, W.G., Jr. (1998). Regulation of hypoxia-inducible mRNAs by the von Hippel-Lindau tumor suppressor protein requires binding to complexes containing elongins B/C and Cul2. *Mol. Cell. Biol.* **18**, 732–741.
- Ma, J., and Ptashne, M. (1987). Deletion analysis of GAL4 defines two transcriptional activating segments. *Cell* **48**, 847–853.
- Maleck, K., Levine, A., Eulgem, T., Morgan, A., Schmid, J., Lawton, K.A., Dangl, J.L., and Dietrich, R.A. (2000). The transcriptome of *Arabidopsis thaliana* during systemic acquired resistance. *Nat. Genet.* **26**, 403–410.
- Maleck, K., Neuenschwander, U., Cade, R.M., Dietrich, R.A., Dangl, J.L., and Ryals, J.A. (2002). Isolation and characterization of broad-spectrum disease-resistant *Arabidopsis* mutants. *Genetics* **160**, 1661–1671.
- Marsilio, E., Cheng, S.H., Schaffhausen, B., Paucha, E., and Livingston, D.M. (1991). The T/t common region of simian virus 40 large T antigen contains a distinct transformation-governing sequence. *J. Virol.* **65**, 5647–5652.
- Mou, Z., Fan, W., and Dong, X. (2003). Inducers of plant systemic acquired resistance regulate NPR1 function through redox changes. *Cell* **113**, 935–944.
- Pontier, D., Miao, Z.-H., and Lam, E. (2001). Trans-dominant suppression of plant TGA factors reveals their negative and positive roles in plant defense responses. *Plant J.* **27**, 529–538.
- Redman, J.C., Haas, B.J., Tanimoto, G., and Town, C.D. (2004). Development and evaluation of an *Arabidopsis* whole genome Affymetrix probe array. *Plant J.* **38**, 545–561.
- Ryals, J.A., Neuenschwander, U.H., Willits, M.G., Molina, A., Steiner, H.-Y., and Hunt, M.D. (1996). Systemic acquired resistance. *Plant Cell* **8**, 1809–1819.
- Saha, S., Brickman, J.M., Lehming, N., and Ptashne, M. (1993). New eukaryotic transcriptional repressors. *Nature* **363**, 648–652.
- Sambrook, J., and Russell, D.W. (2001). *Molecular Cloning: A Laboratory Manual*, 3rd ed. (Cold Spring Harbor, NY: Cold Spring Harbor Laboratory Press).
- Sellers, W.R., Novitch, B.G., Miyake, S., Heith, A., Otterson, G.A., Kaye, F.J., Lassar, A.B., and Kaelin, W.G., Jr. (1998). Stable binding

- to E2F is not required for the retinoblastoma protein to activate transcription, promote differentiation, and suppress tumor cell growth. *Genes Dev.* **12**, 95–106.
- Staswick, P.E., Tiryaki, I., and Rowe, M.L.** (2002). Jasmonate response locus JAR1 and several related *Arabidopsis* genes encode enzymes of the firefly luciferase superfamily that show activity on jasmonic, salicylic, and indole-3-acetic acids in an assay for adenylation. *Plant Cell* **14**, 1405–1415.
- Sticher, L., Mauch-Mani, B., and Métraux, J.P.** (1997). Systemic acquired resistance. *Annu. Rev. Phytopathol.* **35**, 235–270.
- Storey, J.D., and Tibshirani, R.** (2003). Statistical significance for genomewide studies. *Proc. Natl. Acad. Sci. USA* **100**, 9440–9445.
- Strahl, B.D., and Allis, C.D.** (2000). The language of covalent histone modifications. *Nature* **403**, 41–45.
- Thompson, J.D., Higgins, D.G., and Gibson, T.J.** (1994). CLUSTAL W: Improving the sensitivity of progressive multiple sequence alignment through sequence weighting, position-specific gap penalties and weight matrix choice. *Nucleic Acids Res.* **22**, 4673–4680.
- Van Loon, L.C., and Van Strien, E.A.** (1999). The families of pathogenesis-related proteins, their activities, and comparative analysis of PR-1 type proteins. *Physiol. Mol. Plant Pathol.* **55**, 85–97.
- Weigel, D., and Glazebrook, J.** (2002). *Arabidopsis: A Laboratory Manual*. (Cold Spring Harbor, NY: Cold Spring Harbor Laboratory Press).
- Willert, K., and Nusse, R.** (1998). Beta-catenin: A key mediator of Wnt signaling. *Curr. Opin. Genet. Dev.* **8**, 95–102.
- Wilson, I.A., Haft, D.H., Getzoff, E.D., Tainer, J.A., Lerner, R.A., and Brenner, S.** (1985). Identical short peptide sequences in unrelated proteins can have different conformations: A testing ground for theories of immune recognition. *Proc. Natl. Acad. Sci. USA* **82**, 5255–5259.
- Xiang, C., Han, P., Lutziger, I., Wang, K., and Oliver, D.J.** (1999). A mini binary vector series for plant transformation. *Plant Mol. Biol.* **40**, 711–717.
- Zhang, Y., Fan, W., Kinkema, M., Li, X., and Dong, X.** (1999). Interaction of NPR1 with basic leucine zipper protein transcription factors that bind sequences required for salicylic acid induction of the *PR-1* gene. *Proc. Natl. Acad. Sci. USA* **96**, 6523–6528.
- Zhang, Y., and Reinberg, D.** (2001). Transcription regulation by histone methylation: Interplay between different covalent modifications of the core histone tails. *Genes Dev.* **15**, 2343–2360.
- Zhang, Y., Tessaro, M.J., Lassner, M., and Li, X.** (2003). Knockout analysis of *Arabidopsis* transcription factors *TGA2*, *TGA5*, and *TGA6* reveals their redundant and essential roles in systemic acquired resistance. *Plant Cell* **15**, 2647–2653.
- Zhou, J.-M., Trifa, Y., Silva, H., Pontier, D., Lam, E., Shah, J., and Klessig, D.F.** (2000). NPR1 differentially interacts with members of the TGA/OBF family of transcription factors that bind an element of the *PR-1* gene required for induction by salicylic acid. *Mol. Plant Microbe Interact.* **13**, 191–202.
- Zhu, Q., Maher, E.A., Masoud, S., Dixon, R., and Lamb, C.J.** (1994). Enhanced protection against fungal attack by constitutive co-expression of chitinase and glucanase genes in transgenic tobacco. *Biotechnology* **12**, 807–812.